The Canadian Mineralogist
Vol. 43, pp. 1781-1796 (2005)

COPPER AND ZINC IN SILICATE AND OXIDE MINERALS IN IGNEOUS ROCKS FROM THE BINGHAM – PARK CITY BELT, UTAH: SYNCHROTRON X-RAY-FLUORESCENCE DATA

DANIEL P. CORE[§], STEPHEN E. KESLER[¶] AND ERIC J. ESSENE

Department of Geological Sciences, University of Michigan, Ann Arbor, Michigan 48109-1063, U.S.A.

ERIC B. DUFRESNE AND ROY CLARKE

Department of Physics, University of Michigan, Ann Arbor, Michigan 48109-1063, U.S.A.

DOHN A. ARMS AND DON WALKO

Argonne National Laboratories, MHATT-CAT, Argonne, Illinois 60439, U.S.A.

MARK L. RIVERS

The University of Chicago, c/o Argonne National Laboratory, 9700 S. Cass Avenue, Bldg. 434/A004,
Argonne, Illinois 60439. U.S.A.

ABSTRACT

Synchrotron X-ray-fluorescence (SXRF) analyses for Cu, Zn and Fe were carried out on magmatic minerals from intrusive and volcanic rocks in the Bingham – Park City Belt, Utah. The main goals of the study were to determine average Cu and Zn contents and zoning patterns in magmatic minerals in order to shed light on the chemical behavior of Cu and Zn during crystallization of the magmas. The combination of low limits of detection and small analytical footprint makes SXRF the preferred method for tests of this type. Results of the study show that the Zn is homogeneously distributed through most ferromagnesian minerals, commonly following Fe, for which it probably substitutes. The distribution of Cu is more complex, and includes Cu-rich patches of as yet unknown mineralogy that are widespread in all minerals. Median Cu and Zn contents for magmatic minerals, estimated excluding the Cu-rich patches, are lower than and higher than, respectively, those of volcanic rocks in the area. Copper thus must have behaved incompatibly, whereas Zn behaved compatibly during magmatic crystallization. Decreasing Cu concentrations from core to rim were observed in biotite from the volcanic rocks, but Cu and Zn zoning is absent in ferromagnesian minerals in the intrusive rocks. Altered rims on biotite in the intrusive rocks are enriched in Cu and locally in Zn thought to reflect post-crystallization migration of a late magmatic vapor phase.

Keywords: synchrotron X-ray fluorescence, copper, zinc, magnetite, biotite, hornblende, clinopyroxene, feldspar, ilmenite, chlorite, granitic rocks, Bingham – Park City Belt, Utah.

SOMMAIRE

Nous avons effectué des analyses par fluorescence X sur synchrotron (SXRF) afin d'établir les teneurs en Cu, Zn et Fe des minéraux magmatiques provenant de roches intrusives et volcaniques de la ceinture de Bingham – Park City, au Utah. Nos buts principaux étaient de déterminer leurs teneurs moyennes en Cu et Zn et d'évaluer la zonation des minéraux magmatiques afin de préciser le comportement de Cu et de Zn au cours de la cristallisation des magmas. La combinaison des faibles seuils de détection et la focalisation du faisceau fait de l'approche SXRF la mieux adaptée dans les évaluations de ce type. Nos résultats montrent que le Zn est réparti de façon homogène dans la plupart des minéraux ferromagnésiens, suivant le fer, élément auquel il substitue tout probablement. La distribution du Cu est plus complexe, et inclut des taches riches en Cu de minéralogie méconnue, répandues dans la plupart des minéraux. Les teneurs médianes en Cu et en Zn des minéraux magmatiques, estimées en excluant les taches cuprifères, sont inférieures à, et supérieures à, respectivement, celles des roches volcaniques dans la région. Le cuivre a donc dû se comporter de façon incompatible, tandis que le Zn était compatible au cours de la cristallisation du magma. Une diminution de la concentration du Cu du coeur vers la bordure des grains est mise en évidence dans la biotite des roches volcaniques, mais il

---

[§] *Present address*: Geoinformatics, PO Box 1675, West Perth, WA 6872, Australia. *E-mail address*: dancore@ozzie.net.au
[¶] *E-mail address*: skesler@umich.edu

n'y a aucune zonation en Cu ou en Zn dans les minéraux ferromagnésiens des roches intrusives. La bordure altérée de la biotite des roches intrusives, enrichie en Cu et localement en Zn, témoignerait de la migration une phase fluide d'origine magmatique suite à la cristallisation du magma.

(Traduit par la Rédaction)

Mots-clés: synchrotron, fluorescence X, cuivre, zinc, magnétite, biotite, hornblende, clinopyroxène, feldspath, ilménite, chlorite, roches granitiques, ceinture de Bingham – Park City, Utah.

INTRODUCTION

Granitic magmas are associated with a wide range of magmatic–hydrothermal ore deposits containing Cu and Zn, and they are considered to be the main source of these metals (*e.g.,* Candela 1989, Burnham 1997). Although many chemical and physical factors affect whether an intrusion can form an ore deposit, one of the most important is the availability of metals when the magmatic vapor phase forms. If metals behave compatibly and partition into crystals or an immiscible sulfide melt in the silicate magma, they will be depleted in the residual magma, and will not be available to enter any late-forming hydrothermal phase. On the other hand, if they behave incompatibly and concentrate in the residual magma, they can partition into the hydrothermal phase and form ore deposits.

Surprisingly little direct information is available on the behavior of transition-metal elements during the crystallization of magmas. Some granitic rocks contain primary sulfide minerals, but they are scarce and have not been shown to have a systematic distribution with respect to crystallization of magmatic silicate and oxide minerals (Banks 1974, 1982, Borrok *et al.* 1999). Concentrations of minor transition elements in magmatic silicate and oxide minerals are low and poorly known, and have not so far yielded much information on the geochemical evolution of these elements in their host magmas. Studies of magmatic minerals based on analysis of mineral separates showed that: (1) Cu and Zn partition into magmatic oxides and ferromagnesian silicates, (2) Cu contents of these minerals vary much more than Zn contents, (3) high Cu contents are associated with Cu mineralization in some but not all areas, and (4) biotite containing chlorite or other alteration phases has higher Cu contents than unaltered biotite (Parry & Nackowski 1963, Al-Hashimi & Brownlow 1970, Lovering *et al.* 1970, Blaxland 1971, Brabec & White 1971, Graybeal 1973, Banks 1974, Kesler *et al.* 1975, Rehrig & McKinney 1976). Electron-microprobe studies of ferromagnesian silicate and oxide minerals are not able to provide significant information on zoning patterns because of the high detection-limits for Cu and Zn (Banks 1974, Willson 1979). Ion-probe (SIMS and PIXE) analyses, which have the advantage of lower detection-limits, show that unaltered mafic silicate minerals contain 2 to 20 ppm Cu, whereas oxide minerals contain up to 200 ppm (Banks 1982, Hendry *et al.* 1982, 1985, Ewart & Griffin 1994, Stimac & Hickmott 1994). However, the relatively large analytical footprint of SIMS and PIXE analyses (several tens of micrometers in diameter) limits the amount of data that can be obtained on zoning patterns for these elements in minerals from most intrusive rocks.

Synchrotron X-ray fluorescence (SXRF) analysis, which was used in this study, combines very low detection-limits with a small analytical footprint, thus allowing detection of zoning patterns in individual mineral phases. In this preliminary evaluation of the method, work focused on silicate and oxide minerals from igneous rocks in the Bingham – Park City Belt (BPCB) in Utah. The BPCB contains the world-class Bingham porphyry copper deposit, as well as numerous other smaller deposits, all of which are closely associated with igneous rocks.

GEOLOGICAL SETTING OF THE INTRUSIVE ROCKS

The Bingham – Park City Belt (BPCB) consists of 15 granitic plutons and coeval dike and volcanic rocks, which crop out in an east–west-trending belt in central Utah that extends from the Oquirrh Mountains on the west through the Wasatch Range in the east (Fig. 1). Samples were obtained from the Soldiers Canyon and Last Change stocks in the Oquirrh Mountains, the Alta, Clayton Peak, Ontario, and Pine Creek stocks in the Wasatch Range, the Ohio Copper dike in the Bingham district, and the Keetley volcanic rocks in the Wasatch Range. The BPCB magmas probably formed by partial melting of lower crust equivalents of the amphibolites in the Little Willow Formation and were emplaced in an extensional tectonic regime (Vogel *et al.* 2001). Metamorphic assemblages, stratigraphic reconstructions, and fluid-inclusion data have been used to estimate emplacement depths ranging from about 11 km for intrusions in the western part of the Wasatch Range to about 1 km on the east (John 1989). Emplacement depths in the Oquirrh Range are considered to have been less than about 2 km (Waite *et al.* 1997).

The intrusive system at Bingham is associated with the Bingham porphyry copper deposit (PCD), the largest in North America (Phillips *et al.* 1997). Intrusive rocks of the BPCB were emplaced between 39.8 and 30.5 Ma, and igneous activity in the Bingham district itself took place near the start of this period, between about 39.8 and 37.6 Ma (Warnaars *et al.* 1978, Deino & Keith 1997, Vogel *et al.* 2001). The main intrusive body at Bingham consists of the interconnected Last Chance

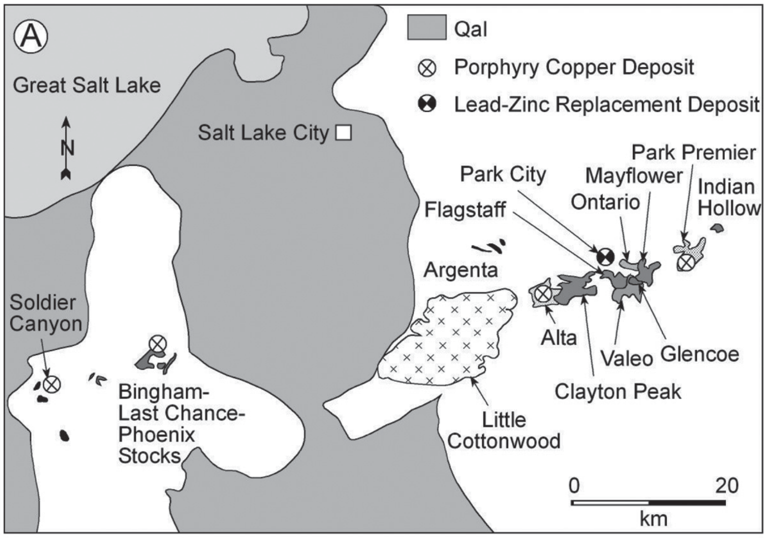

FIG. 1. Map of the Bingham – Park City belt showing the location of intermediate volcanic and plutonic rocks. Also shown are the locations of porphyry Cu deposits and Pb–Zn carbonate replacement deposits.

and Bingham stocks and the Phoenix dike. It has a U–Pb zircon age of 38.6 ± 0.2 Ma and was emplaced before porphyry copper mineralization (Parry *et al.* 2001). The quartz monzonite porphyry (QMP), which is considered to have been associated with the main stage of porphyry copper mineralization at Bingham, crosscuts the Bingham stock and contains zircon with an age of 37.3 ± 0.3 Ma (Core 2004). Three later porphyritic intrusions that are associated with minor Cu mineralization cut the quartz monzonite porphyry, and all intrusive phases are cut by the Ohio Copper dike, which was emplaced following all mineralization. Hydrothermal (alteration) biotite in the quartz monzonite porphyry has a ^{40}Ar/^{39}Ar age of 37.6 ± 0.1 Ma (Parry *et al.* 2001), and molybdenite from veins in the deposit has a Re–Os age of 37.0 ± 0.3 Ma (Chesley & Ruiz 1997, Redmond 2002). Small, uneconomic PCDs are also associated with the Soldiers Canyon stock in the Oquirrh Range, as well as the Alta and Park Premier stocks in the Wasatch Range (John 1989). The K–Ar and Ar–Ar isotope data for the Park Premier deposit suggest that it was roughly coeval with its host stock (John *et al.* 1997). Collectively, the chronological data indicate a close temporal relationship between the porphyry copper deposits and their associated intrusive rocks.

DISTRIBUTION OF CU AND ZN IN IGNEOUS MINERALS

The crystal chemistry of Zn and Cu provides insights about their geochemical behavior. Both Zn and Cu are ordinarily chalcophile elements, and if sufficient reduced sulfur is available in the magma, they form sulfide minerals or a separate sulfide liquid. At high $f(O_2)/f(S_2)$, however, sulfate dominates over sulfide species (Carroll & Rutherford 1988), and most sulfide minerals are not stable (Holland 1959, 1965). Then ferromagnesian silicates and oxides may be able to sequester Zn and Cu into their structures, at least at the 10–100 ppm level. Zinc is generally compatible in ferromagnesian silicates and oxides, such that it partitions into the crystalline solid over a coexisting silicate liquid (Stimac & Hickmott 1994). The ionic radius of Zn^{2+}, Cu^{1+} and Cu^{2+} ions in octahedral sites is on the order of 0.9 Å (Shannon 1976), still able to fit into those sites but large enough to fit less easily.

Copper tends to form covalent bonds in silicates and is excluded from most ferromagnesian silicates. However, tourmaline may have high Cu (Jiang *et al.* 2000), where it substitutes for Al in the *Y* site (MacDonald & Hawthorne 1995). Copper usually occurs in the 1+ valence at $f(O_2)$ below the hematite–magnetite buffer. At more highly oxidizing conditions, Cu may assume 2+ valence, and with its Jahn–Teller behavior, prefers unusual structures with a square planar site such as dioptase, or those with distorted V or VI sites. Both Cu and Zn may partition into spinel structures such as magnetite, where Zn generally prefers the IV over the VI site, and Cu^{2+} enters the VI site in solid solution toward cuprospinel ($CuFe_2O_4$) solid solution (Burns 1993). Experimental studies of magnetite show that Cu substitutes as Cu^{1+} at low levels, whereas at high levels it enters as Cu^{2+} (Sapozhnikova *et al.* 1981).

Zinc readily substitutes into Fe-bearing silicate minerals if it is not sulfidized to form sphalerite. Examples of such substitutions include solid solution of the petedunnite ($CaZnSi_2O_6$) component in clinopyroxene, the $CaZnSi_3O_8$ component in plagioclase, franklinite ($ZnFe_2O_4$) in magnetite, and the hendricksonite component ($KZn_3Si_3AlO_{10}(OH)_2$) in biotite. Zinc can also be found at varying levels in magmatic sulfides. Magmatic sphalerite is rare but has been found as inclusions in phenocrysts from granitic rocks and rhyolites from the Bingham – Park City area (Borrok *et al.* 1999). Zinc also substitutes at low levels into "intermediate solid-solution" (the high-temperature solid-solution in the system Cu–Fe–S near chalcopyrite in composition) and pyrrhotite during crystallization of igneous rocks. Ewart & Griffin (1994) showed that Zn has a partition coefficient greater than one for most silicate and oxide phases, such that it is a compatible element. It strongly favors magnetite, with a partition coefficient as high as 70.

ANALYTICAL METHODS

Synchrotron X-ray fluorescence

Minerals were analyzed by synchrotron X-ray fluorescence (SXRF) using the sector seven beam-line (MHATT–CAT) at the Advanced Photon Source at Argonne National Labs. The relatively low detection-limit of the SXRF method, especially where combined with its analytical footprint of only a few micrometers, allowed analysis of all the silicate minerals for Cu and Zn contents, including those with very low levels (1–10 ppm). Most previous SIMS and other micro-analytical studies focused on analysis of oxides and ferromagnesian silicates, in part because their higher contents of Cu and Zn made them easier to analyze.

Analyses were made on grains in thin sections mounted on Suprasil pure silica glass to avoid contamination from high background-concentrations in normal glass slides. In order to minimize the volume sampled during analyses, thin sections were ground to a thickness of 10 μm. The samples were examined optically, and unaltered grains with clear paragenesis were selected for analysis. The SXRF analyses were made using an X-ray beam with incident energy of 14 kV. The beam was focused to a spot size of approximately 4 μm using Pd-coated mirrors in a Kirkpatrick–Baez (KB) orientation (Kirkpatrick & Baez 1948). The beam was focused on a Nd–YAG crystal, and the light from the fluorescence of the YAG was reflected to a camera. The size of the beam was minimized by adjusting the KB mirrors and monitored by moving a tungsten wire into the path of the beam and monitoring the flux with an ion chamber located behind the wire.

Samples were viewed through a microscope objective with a long working-distance, which was attached to a closed-circuit video system. The beam caused visible fluorescence, allowing determination of its approximate location on the sample. In a few samples, a map of the Fe content in the area of interest was used to provide additional information about the location of spot analyses. This map permitted location of the beam within 5 μm.

Data were collected using a single-element Ge detector placed 8 cm from the sample. A 100 μm high-purity aluminum filter was placed in front of the detector to prevent it from being flooded by the high flux of X-rays. Peak intensities were corrected for absorption by the Al filter. Spectra were collected for 120 s, and background subtraction was done using MCApro (Smith & Rivers 1995). Concentrations of Cu and Zn were determined using Fe as an internal standard. Ratios of Cu to Fe were calculated using the method of Criss (1977). Detection limits for Cu were between 0.1–0.5 ppm for silicates and 5–10 ppm for oxides, depending on the Fe content of the mineral. The precision of these analyses is generally less than 2% at two-sigma limits. Additional errors are introduced from using an internal standard, but two-sigma accuracy should be better than 10%. In addition to point analyses, traverses and maps were made on a few grains. Step sizes of 2 and 5 μm were used for traverses and maps, respectively. The $K\alpha$ peaks of the elements were monitored for 1–2 seconds on each step.

Electron-microprobe analysis

The major-element composition of all spots that were analyzed by SXRF was also measured by electron-microprobe analysis (EMPA) using a Cameca SX100 electron microprobe at the University of Michigan. All minerals were analyzed for Na, Mg, Al, Si, Ca, K, Ti, Mn, Fe and Ba at an operating voltage of 15 kV and a sample current of 10 nA. A focused beam was rastered on a 5 μm spot to minimize beam damage and element migration and to mimic the size of the SXRF beam. The results are not exactly comparable because the EMPA beam has an analytical depth of only 1–2 μm, primarily depending on the excitation voltage of the X-ray line being used for analysis, whereas the SXRF beam enables an analysis from the entire 10 μm thickness of the thin section. Natural and synthetic oxide and silicate minerals were used as standards. Counting times were 20 s for all elements except Fe, which was counted for 40 s.

DISCUSSION OF THE ANALYTICAL RESULTS

Average concentrations and distributions

Our analytical results show that magnetite has the highest average Cu content of any magmatic mineral, followed in order of declining Cu content by biotite, hornblende, pyroxene, ilmenite and feldspar (Table 1). Magnetite also has the highest average Zn content, more than an order of magnitude higher than that for Cu, followed in order of declining Zn content by biotite, ilmenite, pyroxene, and feldspar. The only late-stage mineral that we analyzed is chlorite, which appears to have formed by alteration of ferromagnesian minerals. In most samples, chlorite is scarce and forms grains that are too small to be analyzed separately by the SXRF beam. In two samples from the Alta stock, however, chlorite forms large, solitary grains that are similar in size to biotite and which could be analyzed. Results from these two samples show that chlorite has highly variable Cu contents that are generally higher than those of unaltered biotite in the same rock, whereas the Zn contents are similar to those in biotite (Table 1).

Average Cu concentrations in Table 1 are somewhat misleading, however, because distributions of Cu concentrations for most minerals are bimodal, even if plotted on a geometric scale (Fig. 2). In contrast, Zn concentrations are largely unimodal with a few anomalous high values if plotted on an arithmetic scale (Fig. 2), making the arithmetic averages more useful. This difference in the distribution of Cu and Zn in the rocks results from the presence of Cu-rich patches in most of the minerals. Figure 3, which is an X-ray map of a biotite grain from the Clayton Peak stock (CP13–14), shows this phenomenon. Whereas Zn and Fe have similar, smooth variations in concentration in the biotite, Cu is strongly enriched in patches at a 10 to 50 μm scale inside the grains, as well as along the rims of grains. Similar Cu-rich patches are present in most other minerals that were analyzed, including magnetite and feldspar, and they are more common in the intrusive rocks and less common in the Keetley volcanic rocks.

The identity of these Cu-rich zones is not fully understood. No features could be correlated with the Cu-rich zones in either high-magnification optical microscopy or SEM images, making it very unlikely that they are simple mineral or fluid inclusions. Extremely small, submicroscopic inclusions cannot be ruled out, but the relatively large size of the Cu-rich patches

TABLE 1. AVERAGE AND RANGE OF Cu AND Zn CONCENTRATIONS IN SILICATE AND OXIDE MINERALS FROM IGNEOUS ROCKS IN THE BINGHAM – PARK CITY BELT, UTAH

	All grains (ave.)	All grains (range)	# of anal.	High Cu (ave.)	High Cu (range)	# of anal.	Low Cu (ave.)	Low Cu (range)	# of anal.
				Magnetite					
Cu	210	6-1900	39	800	50-1900	9	30	6-95	30
Zn	2400	90-7800	39	3600	380-5900	9	2050	90-7800	30
				Biotite					
Cu	120	1-2700	77	200	10-2700	42	15	1-75	35
Zn	790	470-1190	77	840	540-1190	42	730	470-960	35
				Hornblende					
Cu	40	2-200	33	100	40-200	11	10	2-60	22
Zn	480	220-750	33	450	310-750	11	490	220-700	22
				Clinopyroxene					
Cu	30	2-120	22	70	30-120	8	8	2-19	14
Zn	380	200-610	22	390	310-560	8	360	200-610	14
				Feldspar					
Cu	23	1-460	33	80	15-460	8	5	1-11	28
Zn	18	3-43	33	27	6-44	8	15	3-28	28
				Ilmenite					
Cu	22	5-53	7						
Zn	550	430-1100	7						
				Chlorite					
Cu	250	27-570	4						
Zn	1300	1200-1500	4						

All analyses by synchrotron X-ray fluorescence; all results quoted in parts per million.

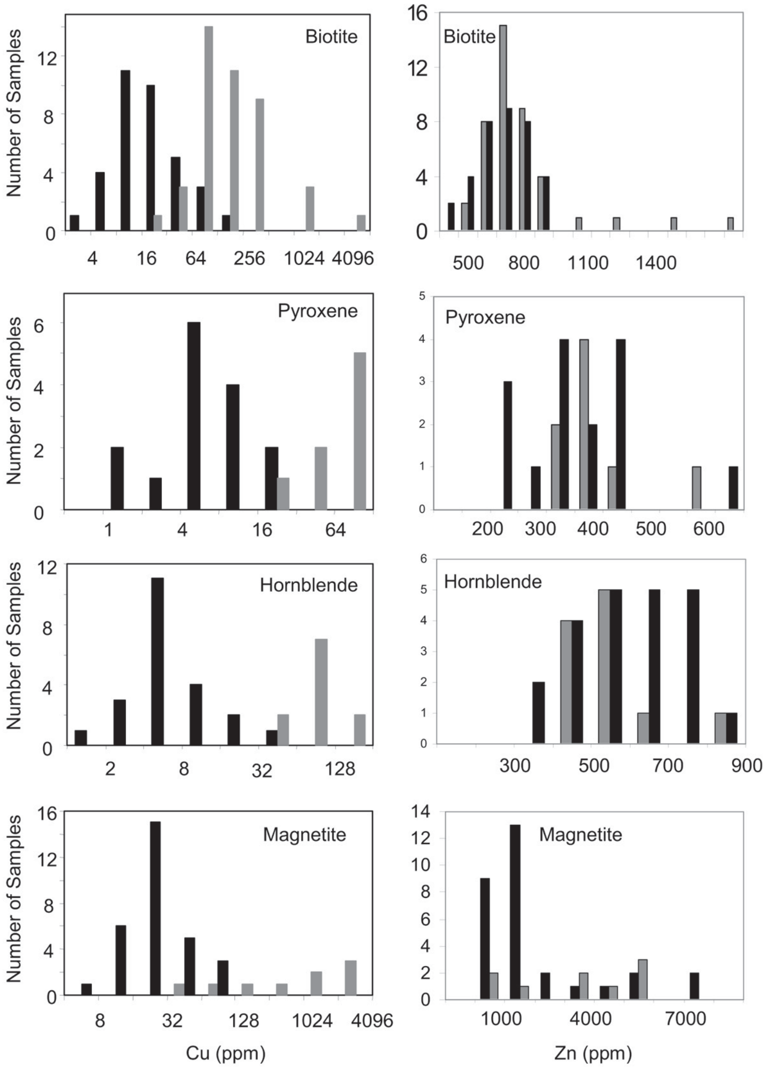

FIG. 2. Histograms showing abundance distributions for Cu and Zn in biotite, pyroxene, hornblende and magnetite from the Bingham – Park City Belt. Data are divided into high-Cu (gray) and low-Cu (black) groups, as discussed in the text.

makes this seem unlikely. Banks (1974, 1982) also observed Cu enrichment in mafic minerals, especially biotite, and suggested that it is due to the presence of chlorite or related alteration-induced minerals. Chlorite was not observed in the Cu-rich patches within minerals analyzed in this study, however. Li *et al*. (1998) found with TEM studies that partially chloritized biotite contains Cu sulfides, which they suggested formed by introduction of Cu and S during hydrothermal activity rather than by isochemical oxidation-reduction reactions, but we did not observe any sulfide inclusions in the Cu-rich patches. Furthermore, although we could not measure S concentrations in the SXRF analyses, Fe concentrations that would reflect the presence of chalcopyrite or bornite were measured, and they do not co-vary with Cu concentrations (Fig. 3). Ilton & Veblen (1988, 1993) have described biotite with expanded layers that contain native Cu, another possible host for Cu. However, we did not observe native Cu inclusions, and the native Cu described by Ilton & Veblen probably formed during oxidative weathering, which did not affect our samples.

In view of the patchy distribution of Cu in these minerals, we divided our analytical results for Cu into “high-Cu” compositions from Cu-rich patches and “low-Cu” compositions from surrounding areas of each grain. High-Cu zones were found by making traverses across the grains and locating areas with anomalous Cu values. Because background abundances of Cu vary from mineral to mineral and from grain to grain, the minimum concentration of Cu necessary for a zone to be classified as high-Cu also varied, even for individual mineral groups such as biotite. As a result, high-Cu and low-Cu populations overlap if Cu concentrations are plotted for all compositions of each mineral (Fig. 2). Table 1 summarizes average Cu and Zn contents of high- and low-Cu zones, along with the range of values in each group. Table 1 also shows that average Zn contents are slightly higher in the high-Cu groups for magnetite, biotite, pyroxene and feldspar, but not for hornblende.

Figure 4 shows Cu–Fe, Cu–Zn and Zn–Fe scatter plots for the main minerals analyzed in this study, with data divided into high-Cu and low-Cu categories. The Cu–Zn relations are entirely random for biotite, hornblende and pyroxene, whereas there is a weak positive correlation for magnetite and feldspar. The Cu–Fe plots are random for biotite, hornblende and pyroxene, and show a weak negative correlation for magnetite, reflecting the high Ti content of magnetite in the high-Cu compositions, and a weak positive correlation for feldspar. The Zn–Fe plots show a strong positive correlation for hornblende and feldspar and probable positive correlations for biotite and pyroxene that may

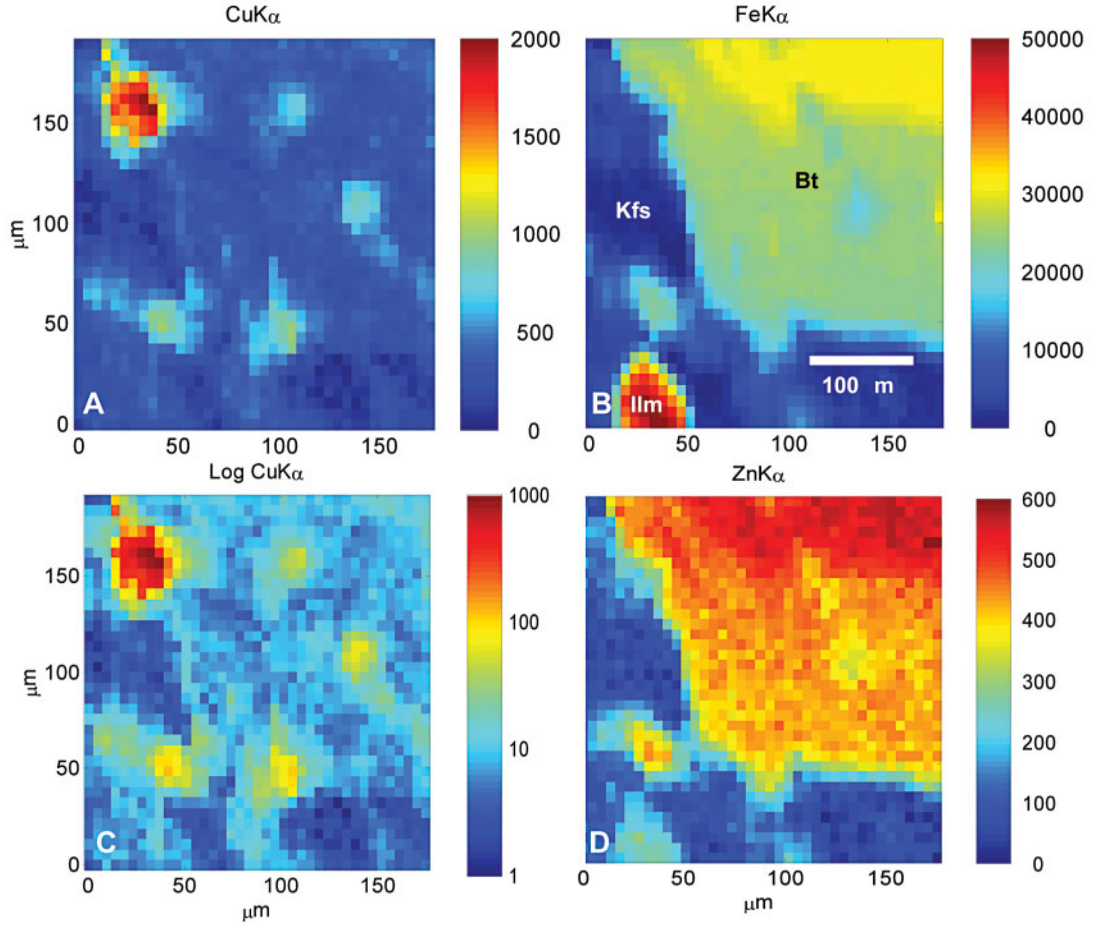

FIG. 3. X-ray maps of biotite grain from Clayton Peak stock (CP13–14). A) Cu*K*α map showing Cu-rich patches in the biotite grain and on the rim of the grain, B) Fe*K*α map showing distribution of phases that are present. C) Log Cu*K*α map, which provides a better indication of the variation in Cu around the Cu-rich patches. D) Zn*K*α map. All maps are based on results of individual analyses at each of the pixels in this image.

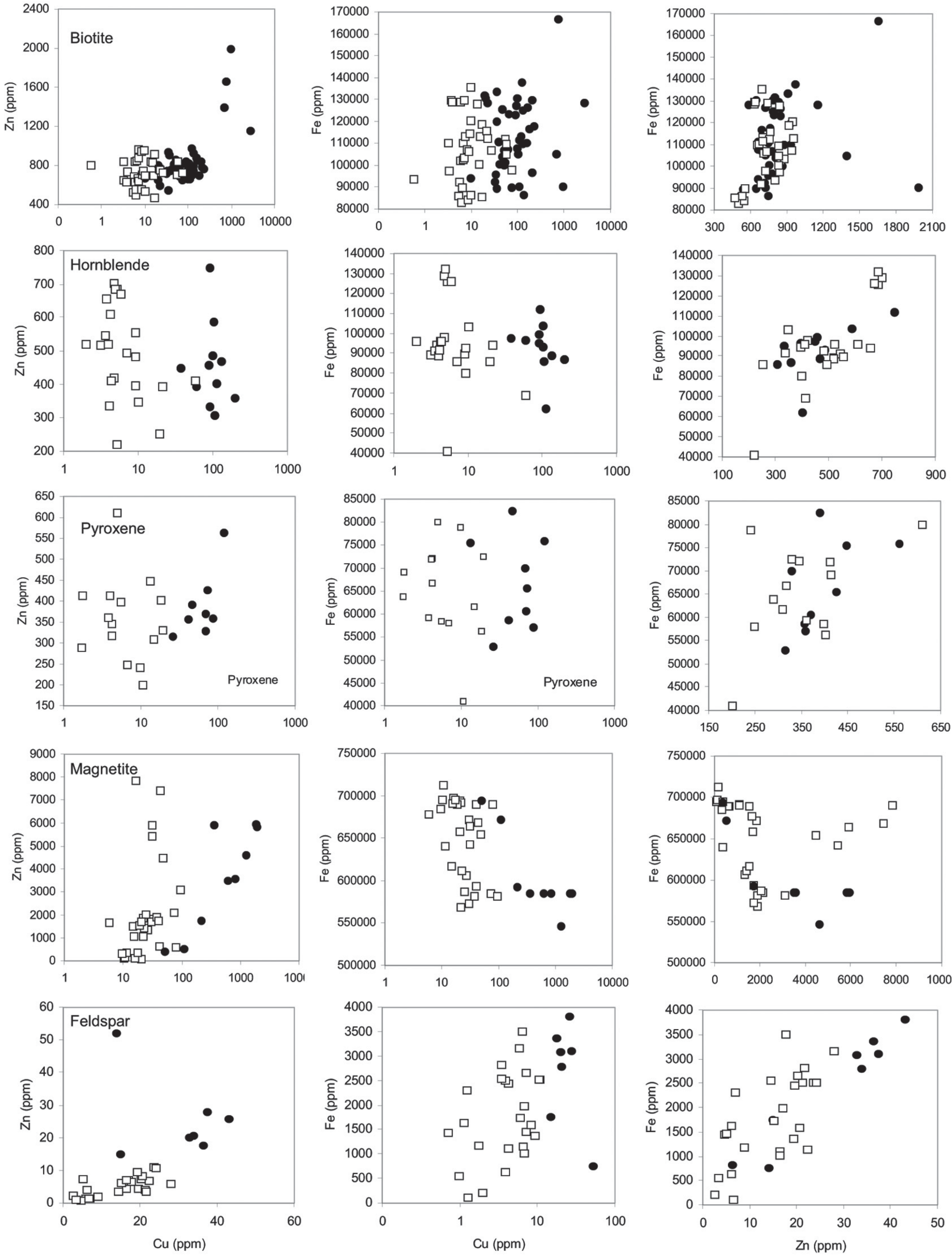

FIG. 4. Cu–Zn, Cu–Fe and Fe–Zn relations for biotite, hornblende, pyroxene, magnetite and feldspar from intrusive igneous rocks of the Bingham – Park City Belt. Note that Cu is plotted on a logarithmic axis, and Zn and Fe are plotted on arithmetic axes. Samples are shown as squares (low-Cu zones) and filled circles (high-Cu zones).

reflect substitution of Zn for Fe. Magnetite shows a more complex pattern but a good positive correlation for high Fe and Zn concentrations, also suggesting substitution of Zn for Fe.

Sulfidation–oxidation reactions governing substitution of Cu and Zn in silicate and oxide minerals

Our analytical data can be used to provide some insights into the behavior of Cu and Zn during magmatic crystallization. According to conventional wisdom, ore elements should concentrate in the residual magma (behave incompatibly) and then separate into a late hydrothermal phase that forms ore deposits. On the other hand, if the ore elements behave compatibly by entering a mineral that forms during magmatic crystallization, a late-forming hydrothermal phase might be poor in these ore elements. Magmatic sulfide minerals could be very important hosts for ore elements if they formed early in the crystallization history and were sufficiently abundant. However, Borrok *et al.* (1999) showed that sulfides are relatively scarce in the BPCP intrusive rocks, suggesting that substitution of ore elements into silicate and oxide minerals could be important.

Reactions involving oxygen and sulfur fugacities and sulfide-bearing assemblages, which buffer the substitution of Cu and Zn into silicate and oxide minerals, provide insight into the conditions that govern this substitution. For instance, if magmatic sphalerite is present, petedunnite substitution in clinopyroxene is buffered by:

$$2\ \mathrm{CaZnSi_2O_6} + 2\ \mathrm{S_2} = 2\ \mathrm{ZnS} + 2\ \mathrm{CaSiO_3} + 2\ \mathrm{SiO_2} + \mathrm{O_2}$$

(Essene & Peacor 1987). In the absence of wollastonite and in the presence of orthopyroxene and augite, it would be buffered by:

$$2\ \mathrm{CaZnSi_2O_6} + 2\ \mathrm{FeSiO_3} + 2\ \mathrm{S_2} = 2\ \mathrm{ZnS} + 2\ \mathrm{CaFeSi_2O_6} + 2\ \mathrm{SiO_2} + \mathrm{O_2}$$

$$2\ \mathrm{CaZnSi_2O_6} + 2\ \mathrm{FeSiO_3} + 2\ \mathrm{S_2} = 2\ \mathrm{ZnS} + 2\ \mathrm{CaFeSi_2O_6} + 2\ \mathrm{SiO_2} + \mathrm{O_2}$$

Two-pyroxene assemblages occur in some of the granitic rocks under study (Core 2004), and these reactions could be calculated from the available data. Thermodynamic and mixing data for petedunnite in clinopyroxene could be derived using in part the experimental data (Rothkopf & Fehr 1998) to allow calibration of these reactions in $f(\mathrm{S_2})$–$f(\mathrm{O_2})$ space at a fixed P–T. However, in the absence of sphalerite, they provide only a limit to oxygen and sulfur fugacities. Ionic equilibria could also be considered in the presence of a vapor phase, such as:

$$\mathrm{CaZnSi_2O_6} + \mathrm{Fe^{2+}} = \mathrm{CaFeSi_2O_6} + \mathrm{Zn^{2+}}$$

The composition of the pyroxene could be contoured on a diagram of $\log(a\mathrm{Zn^{2+}})/\log(a\mathrm{Fe^{2+}})$ *versus* T at a fixed P. If the activity of $\mathrm{Fe^{2+}}$ in the parent magma can be estimated, the amount of $\mathrm{Zn^{2+}}$ that should also be present could also be estimated.

Substitution of Zn in feldspar may be understood relative to the synthetic phase $\mathrm{CaZnSi_3O_8}$, which has a feldspar structure. Derivation of its thermodynamic properties from the experiments of Fehr & Huber (2001) and application of a selected thermodynamic model would allow calculation of reactions based on:

$$2\ \mathrm{CaZnSi_3O_8} + 2\ \mathrm{S_2} = 2\ \mathrm{ZnS} + 2\ \mathrm{CaSiO_3} + 4\ \mathrm{SiO_2} + \mathrm{O_2}$$

$$2\ \mathrm{CaZnSi_3O_8} + 2\ \mathrm{MgSiO_3} + 2\ \mathrm{S_2} = 2\ \mathrm{ZnS} + 2\ \mathrm{CaMgSi_2O_6} + 4\ \mathrm{SiO_2} + \mathrm{O_2}$$

$$2\ \mathrm{CaZnSi_3O_8} + 2\ \mathrm{FeSiO_3} + 2\ \mathrm{S_2} = 2\ \mathrm{ZnS} + 2\ \mathrm{CaFeSi_2O_6} + 4\ \mathrm{SiO_2} + \mathrm{O_2}$$

The latter two reactions would apply in the presence of the assemblage plagioclase – clinopyroxene – orthopyroxene – quartz – sphalerite. Franklinite and cuprospinel substitutions in magnetite are buffered by reactions such as the following:

$$6\ \mathrm{ZnFe_2O_4} + 3\ \mathrm{S_2} = 6\ \mathrm{ZnS} + 4\ \mathrm{Fe_3O_4} + 4\ \mathrm{O_2}$$

$$3\ \mathrm{CuFe_2O_4} + 3\ \mathrm{S_2} = 3\ \mathrm{CuFeS_2} + \mathrm{Fe_3O_4} + 4\ \mathrm{O_2}$$

At a given $f(\mathrm{S_2})$ and $f(\mathrm{O_2})$, sphalerite buffers the franklinite substitution in magnetite, and chalcopyrite or bornite buffer the proportion of cuprospinel in magnetite. Bornite is a magmatic mineral in some oxidized granitic rocks (Core 2004). The Cu content of magnetite in equilibrium with bornite will constrain oxygen and sulfur fugacities if a mixing model for cuprospinel–magnetite is available and the composition of magmatic bornite can be recovered. Experimental data in the system $\mathrm{CuFe_2O_4}$–$\mathrm{Fe_3O_4}$ (Katkov & Lykasov 2003) provide information on the mixing properties for this binary system. However, at minor levels, Cu substitutes in magnetite *via* $\mathrm{Cu^{1+}} + \mathrm{Fe^{3+}} = 2\ \mathrm{Fe^{2+}}$ (Sapozhnikova *et al.* 1981). The following reactions apply:

$$5\ \mathrm{CuFe_2O_4} + 2\ \mathrm{S_2} = \mathrm{Cu_5FeS_4} + 3\ \mathrm{Fe_3O_4} + 4\ \mathrm{O_2}$$

$$6\ \mathrm{Cu_{0.5}Fe_{2.5}O_4} + 3\ \mathrm{S_2} = 3\ \mathrm{CuFeS_2} + 4\ \mathrm{Fe_3O_4} + 4\ \mathrm{O_2}$$

$$10\ \mathrm{Cu_{0.5}Fe_{2.5}O_4} + 2\ \mathrm{S_2} = \mathrm{Cu_5FeS_4} + 8\ \mathrm{Fe_3O_4} + 4\ \mathrm{O_2}$$

The slopes and positions of these reactions in $f(\mathrm{S_2})$ – $f(\mathrm{O_2})$ space thus depend on both the valence and amount of Cu in magnetite in equilibrium with sulfide. The valence of Cu in magnetite and the other phases from oxidized granitic rocks needs to be determined before quantitative values of oxygen and sulfur fugacity are extracted from the observed levels of Cu in the minerals.

Zinc is buffered in biotite with K-feldspar and sphalerite *via* the reaction:

$$2\ KZn_3Si_3AlO_{10}(OH)_2 + 3\ S_2 = 2\ KAlSi_3O_8 + 6\ ZnS + 2\ H_2O + 3\ O_2.$$

At present this reaction cannot be quantified, although observations of the Zn level in biotite from granites for which $f(S_2) - f(O_2) - P(H_2O) - T$ have been estimated could be used to derive a fictive value for the ΔG of hendricksonite, depending on the mixing model that was employed as well as the accuracy of $f(S_2) - f(O_2)$ and thermobarometry. Copper in biotite is buffered as Cu^{2+} in the presence of bornite – sanidine – fluid by:

$$5\ KCu^{2+}{}_3Si_3AlO_{10}(OH)_2 + KFe_3Si_3AlO_{10}(OH)_2 + 6\ S_2 = 6\ KAlSi_3O_8 + 3\ Cu_5FeS_4 + 6\ H_2O + 9\ O_2$$

and with bornite – magnetite – sanidine – fluid by:

$$10\ KCu^{2+}Fe_2Si_3AlO_{10}(OH)_2 + 4\ S_2 = 10\ KAlSi_3O_8 + 2\ Cu_5FeS_4 + 6\ Fe_3O_4 + 10\ H_2O + 3\ O_2$$

Similar reactions may be balanced with chalcopyrite. However, different reactions buffer Cu^{1+} in biotite with bornite and magnetite:

$$10\ KCu^{1+}{}_{0.5}Fe^{3+}{}_{0.5}Fe^{2+}{}_2Si_3AlO_{10}(OH)_2 + 2\ S_2 = 10\ KAlSi_3O_8 + Cu_5FeS_4 + 8\ Fe_3O_4 + 10\ H_2O + 3\ O_2$$

Application of these and related reactions await careful experiments establishing both the valence and level of substitution of Cu in biotite and chlorite. Yet other reactions may be postulated for Zn and Cu in hornblende and also in chlorite if they actually substitute in the structure rather than representing submicroscopic contaminants of metals or sulfides.

Significance of the results to ore-forming processes

Sulfidation relations, combined with the results of Borrok *et al.* (1999) and our analytical data, show that sulfide minerals are not the dominant host for Cu and Zn in the BPCB rocks. Thus, their behavior during crystallization was probably controlled by crystallization of silicate and oxide minerals. In order to evaluate whether these elements behaved compatibly or incompatibly during crystallization, we need to compare the Cu and Zn contents of minerals in the intrusive rocks to the Cu and Zn contents of their parent magmas. Although we do not know the Cu and Zn contents of the parent BPCP magmas, the Keetley volcanic rocks from the BPCB have Cu contents of 10 to 20 ppm and Zn contents of 40 to 65 ppm, which are typical of most igneous rocks (Thomas Vogel, written commun., 2005).

The unaltered silicate minerals analyzed in our study have a median Cu content of less than 10 ppm Cu. Oxide minerals are slightly more enriched in Cu with around 20 ppm as a median value in areas that are not "Cu-rich". These concentrations are equal to or lower than those of Keetley volcanic rocks, suggesting that Cu behaved incompatibly and was concentrated in the BPCB magmas. The Zn contents of mafic silicate and oxide minerals (500 to 1000 ppm) are considerably higher than values typical of the volcanic rocks, suggesting that crystallization of mafic minerals in the BPCB magmas depleted the remaining melt in Zn. This is consistent with the abundance of Cu mineralization associated with the BPCB intrusions. According to the summaries of John (1997) and Babcock *et al.* (1997), Cu and Zn production from Bingham and Park City, the two dominant mining districts in the area, have been about 2.36 × 10^9 and 2.27 × 10^9 kg, respectively for a Cu/Zn (weight) ratio of about 9.6, which is about one order of magnitude larger than the ratio of Cu and Zn crustal abundances of about 0.94 (Taylor & McLennan 1985). This provides a rough indication of the degree to which Cu was concentrated relative to Zn during the formation and crystallization of the BPCB magmas.

Zoning patterns in single minerals may provide further information on whether Cu and Zn behaved compatibly or incompatibly during crystallization of the BPCB magmas. Increased concentration of either element toward the rim of individual grains would indicate incompatible behavior. As a simple test of this, we analyzed the core and rim of individual silicate and oxide grains. Pairs of results for core and rim of individual grains of magnetite, biotite and pyroxene are compared in Figure 5. For magnetite and biotite, more Cu data points fall above the lines indicating equal concentrations than fall below them, suggesting widespread but not consistent enrichment in the rim, which would be predicted for incompatible behavior. The data points for Zn show a generally similar though weaker pattern, however, that was not predicted from the average concentrations. For pyroxene, a few more Cu and Zn data-points plot below the rims, suggesting that it recorded decreasing Cu and Zn contents (provided that other factors affecting Cu and Zn uptake by these minerals were constant). We also analyzed along traverses from the core to the rim in a few individual grains. The only traverse that showed a clear pattern of zoning was from a biotite grain in the Keetley volcanic rocks, in which the Cu content of the grain increased toward the edge of the grain, as might result from incompatible behavior, whereas Zn is almost unchanged (Fig. 6). Results along other traverses did not show a consistent pattern. These variable results might reflect the fact that individual minerals did not crystallize over a sufficiently long interval to record large changes in the Cu or Zn content of their parent magmas, or that

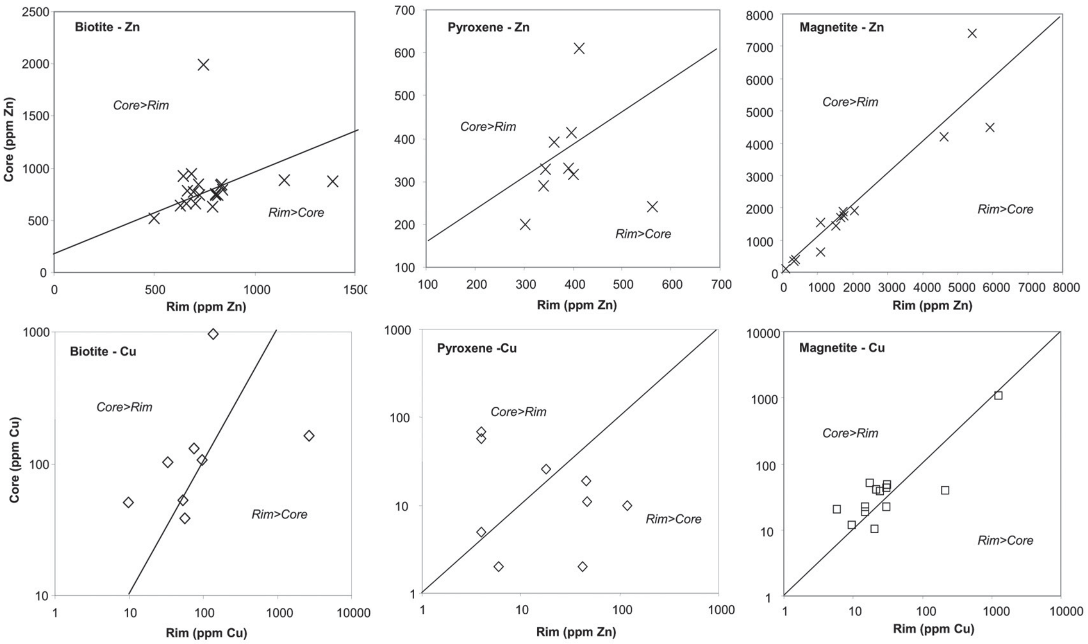

FIG. 5. Comparison of Cu and Zn data for cores and rims of individual grains of magnetite, biotite and pyroxene. Lines in each diagram are for equal concentrations of the elements in cores and rims. Results that plot about the line pertain to grains in which the rims are enriched in Cu or Zn and those that plot below the line are for grains in which the rims are depleted in Cu or Zn.

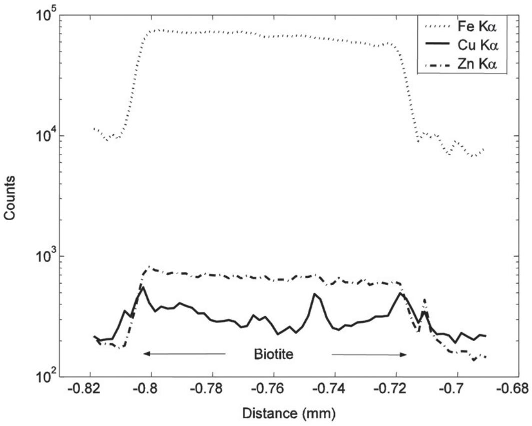

FIG. 6. Traverse across biotite grain from the Keetley volcanic unit showing counts on the Fe, Cu, and Zn*K*α lines. Zoning shows gradual increase in Cu from core to rim, and Zn following Fe with a relatively flat profile.

compatible *versus* incompatible behavior of Cu or Zn changed with time during crystallization of the magmas. Considerably more analyses will need to be performed to test either possibility.

The BPCB hosts the large Bingham porphyry copper deposit (PCD), and it is a good setting in which to test the relation between fertile and barren intrusions, *i.e.*, those that are associated with ore deposits and those that are not. The Last Chance stock was emplaced immediately before formation of the Bingham deposit and is classified here as a fertile intrusion. The Soldier Canyon, Alta and Park Premier stocks, which are associated with small and uneconomic PCD prospects, are included here in the barren category; no intrusion has been directly associated with the Park City Zn–Pb–Ag district (John 1997). This classification is obviously subject to uncertainties about age of intrusive rocks and ore deposits and to accidents of exposure. Table 2, which provides summary statistics for BPCB igneous rocks divided into fertile and barren categories, shows that average Cu concentrations in clinopyroxene, hornblende, biotite and magnetite from the fertile Last Chance intrusion are consistently lower than those from the barren intrusions. For all minerals, the range of Cu contents for the barren intrusions extends to higher values than does the range for the fertile (Last Chance) intrusion. The paucity of analyses from the fertile Last Chance intrusion makes these comparisons suspect for magnetite and hornblende, but comparisons for clinopyroxene and biotite involve similar numbers of samples and are more convincing. The best mineral for direct comparisons is probably clinopyroxene, which formed early in the crystallization sequence and therefore would be most likely to reflect the composition of the original magma. Figure 7 shows that Cu contents for clinopyroxene in the fertile samples are bimodal. Even with this complication, the average Cu content of the fertile samples is lower than that of the barren samples. This result supports suggestions that formation of large PCDs depletes their parent magma system in Cu.

One unusual feature of the intrusive rocks that was observed during our analyses is the tendency for Cu and, less commonly, Zn to be strongly enriched along the rim of some biotite grains (Fig. 8). Figure 9 shows that these enriched rims consist largely of chlorite and titanite, although variable amounts of magnetite and K-feldspar were found in other rims. These minerals are typical of PCD alteration assemblages and almost certainly reflect postmagmatic migration of hydrothermal solutions along intergranular zones in the intrusive rock. Reconnaissance laser-ablation, inductively coupled plasma – mass spectrometric (LA–ICP–MS) analyses of these grains of biotite show that the Cu-rich rims are widespread, suggesting that they formed from processes that affected large parts of their host intrusions. Observations on fluid inclusions in porphyry copper deposits have been interpreted to suggest that a low-density vapor phase moves upward from an underlying magma chamber into shallower areas before actually forming the ore zones (Redmond *et al.* 2004). The degree to which these fluids interact with surrounding rocks through which they pass remains unclear, but they might form these Cu-rich altered rims. If this is the case, systematic surveys of the distribution of these altered rims might be used to map flow paths of Cu-rich fluids through otherwise barren rocks, providing new information on the flow patterns of magmatic fluids and allowing a test of these newly developed models.

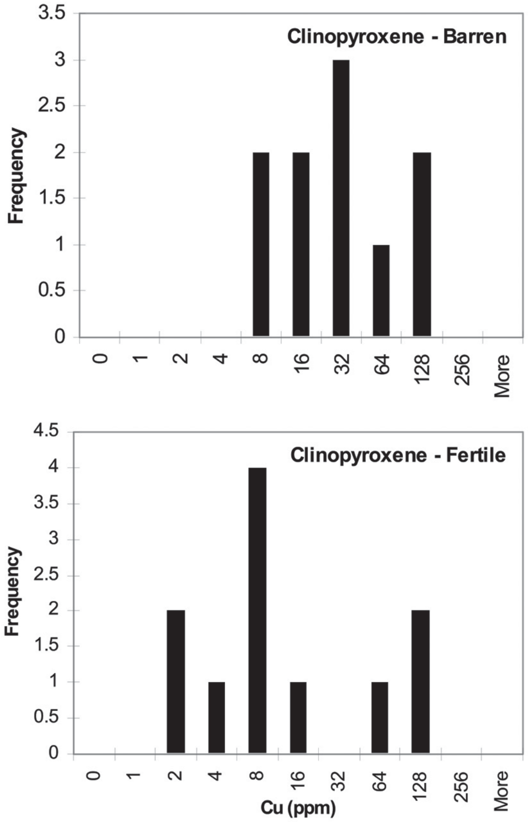

FIG. 7. Frequency diagram showing distribution of Cu contents of clinopyroxene from fertile (Last Chance) and barren (all other rock units) igneous rocks in the BPCB.

CONCLUSIONS

Our results show that analyses by synchrotron X-ray fluorescence can be used to determine the Cu and Zn contents of igneous minerals, and that these elements are present in two forms, one of which is clearly magmatic in origin. The other form consists of patches and altered rims and at least partly reflects later alteration. Concentrations of Cu and Zn that are interpreted to be of magmatic origin are less than and greater than those of probably parent magmas, respectively, indicating that Cu behaved incompatibly, whereas Zn behaved compatibly during crystallization of the host magmas. Variations in the concentration of Cu and Zn that might reflect magmatic ore-forming processes were not observed, although concentrations of Cu on altered margins of biotite appear to reflect passage of a Cu-rich fluid and might be used as a vector toward areas of mineralization.

TABLE 2. SUMMARY STATISTICS FOR Cu CONTENTS OF MINERALS IN THE BPCB IGNEOUS ROCKS DIVIDED INTO A FERTILE GROUP, CONSISTING OF THE LAST CHANCE STOCK, AND A BARREN GROUP THAT INCLUDES MOST OTHER INTRUSIONS

Group	Mineral	Cu (ave.)	Cu (range)	*n*
Fertile	Clinopyroxene	20	17 - 72	11
Barren	Clinopyroxene	36	2 - 120	11
Fertile	Hornblende	5	2 - 9	2
Barren	Hornblende	42	2 - 200	31
Fertile	Biotite	88	1 - 960	20
Barren	Biotite	125	4 - 2700	57
Fertile	Magnetite	31	22 - 41	2
Barren	Magnetite	220	6 - 1900	37

All values in ppm; *n*: number of analyses made.

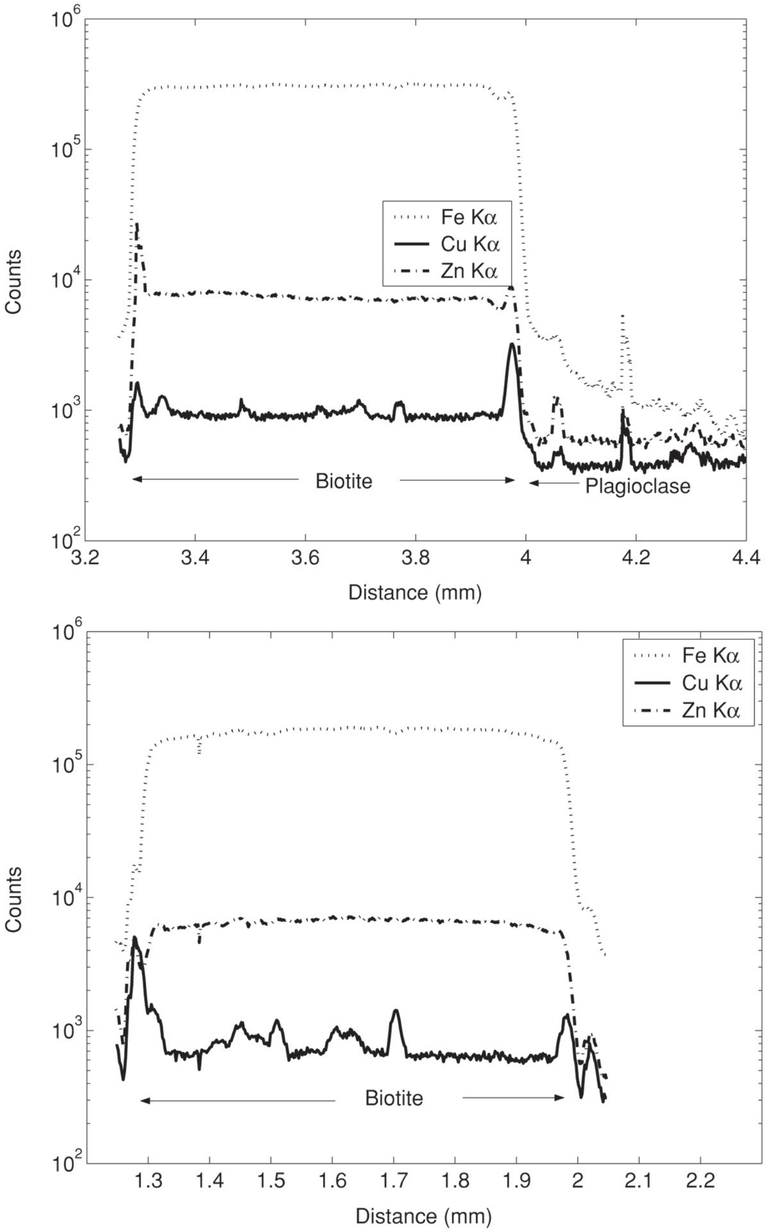

FIG. 8. Traverses across biotite grains showing counts on the Fe, Cu, and Zn*K*α lines. Upper diagram: biotite and plagioclase from the Alta stock (A20–12). Rims of the biotite grain are enriched in both Cu and Zn, and the plagioclase shows patchy zoning of both elements. Lower diagram: biotite from the Pine Creek stock (PC9–6). Rims of the biotite are enriched in Cu, but not Zn. The interior of this grain shows patchy zoning in Cu, whereas Zn follows Fe.

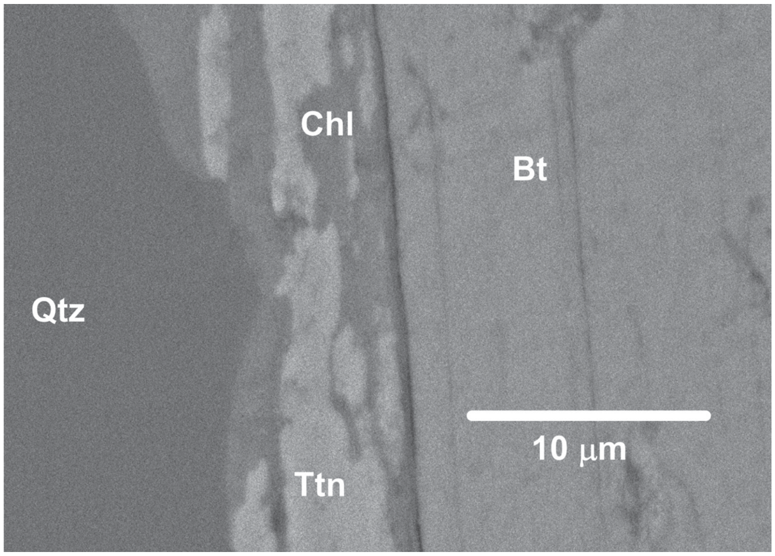

FIG. 9. BSE image of boundary of biotite grain in sample A20–12 from the Alta stock. Edge of the grain has been altered to a mixture of chlorite and titanite. Other grains show thinner alteration-induced rims that also contain magnetite and K-feldspar.

ACKNOWLEDGEMENTS

We are pleased to have this work included in a volume in honor of Mike Fleet, who was an early user of synchrotron radiation in efforts to characterize minerals. Our report on synchrotron X-ray-fluorescence analyses was funded by BHP–Billiton and by NSF grant EAR–02–30098. Guidance in fieldwork was provided by Patrick Redmond and Ezra Inan of Stanford University, and samples from the Wasatch Range were provided by Thomas Vogel of Michigan State University, who also supplied information on the trace-element content of the rocks. Carl Henderson assisted with the electron-microprobe analyses. Grant Henderson, Thomas Vogel and an anonymous reviewer provided helpful comments on an earlier version of this manuscript.

REFERENCES

AL-HASHIMI, A.R.K. & BROWNLOW, A.H. (1970): Copper content of biotites from the Boulder Batholith, Montana. *Econ. Geol.* **65**, 985-992.

BABCOCK, R.C., BALLENTYNE, G.H. & PHILLIPS, C.H. (1997): Summary of the geology of the Bingham District, Utah. *In* Geology and Ore Deposits of the Oquirrh and Wasatch Mountains, Utah (D.A. John & G.H. Ballantyne, eds.). *Soc. Econ. Geol., Guidebook Ser.* **29**, 113-132.

BANKS, N.G. (1974): Distribution of Cu in biotite and biotite alteration products in intrusive rocks near two Arizona porphyry copper deposits. *J. Res. U.S. Geol. Surv.* **2**, 195-211.

________ (1982): Sulfur and copper in magma and rocks: Ray porphyry copper deposit, Pinal County, Arizona. *In* Advances in Geology of Porphyry Copper Deposits, Southwestern North America (S.R. Titley, ed.). University of Arizona Press, Tucson, Arizona (227-257).

BLAXLAND, A.B. (1971): Occurrence of zinc in granitic biotites. *Mineral. Deposita* **6**, 313-320.

BORROK, D., KESLER, S.E., ESSENE, E.J. & VOGEL, T.A. (1999): Sulfide mineral in intrusive and volcanic rocks of the Bingham – Park City Belt, Utah. *Econ. Geol.* **94**, 1213-1230.

BRABEC, D. & WHITE, W.H. (1971): Distribution of copper and zinc in rocks of the Guichon Creek Batholith, British Columbia. *Can. Inst. Mining Metall., Spec. Vol.* **11**, 291-297.

BURNHAM, C.W. (1997): Magmas and hydrothermal fluids. *In* Geochemistry of Hydrothermal Ore Deposits (H.L. Barnes, ed.). John Wiley and Sons, New York, N.Y. (63-125).

BURNS, R.G. (1993): *Mineralogical Applications Of Crystal Field Theory* (2nd ed.). Cambridge University Press, Cambridge, U.K.

CANDELA, P.A. (1989): Magmatic ore-forming fluids; thermodynamic and mass transfer calculations of metal concentrations. *In* Ore Deposition Associated with Magmas

(J.A. Whitney & A.J. Naldrett, eds.). *Rev. Econ. Geol.* **4**, 203-221.

Carroll, M.R. & Rutherford, M.J. (1988): Sulfur speciation in hydrous experimental glasses of varying oxidation state; results from measured wavelength shifts of sulfur X-rays. *Am. Mineral.* **86**, 845-849.

Chesley, J.T. & Ruiz, J. (1997): Preliminary geochronology on molybdenite mineralization from the Bingham Canyon ore deposit, Utah. *In* Geology and Ore Deposits of the Oquirrh and Wasatch Mountains, Utah (D.A. John and G.H. Ballantyne, eds.). *Soc. Econ. Geol., Guidebook Ser.* **29**, 282.

Core, D.P. (2004): *Oxygen and Sulfur Fugacities of Granitoids: Implications for Ore-Forming Processes.* Ph.D. dissertation, University of Michigan, Ann Arbor, Michigan.

Criss, J.W. (1977): NRLXRF, A Fortran program for X-ray fluorescence analysis: Users' Reference Manual and General Documentation, COSMIC DOD-00065.

Deino, A., & Keith, J.D. (1997): Ages of volcanic and intrusive rocks in the Bingham mining district, Utah. *Soc. Econ. Geol., Guidebook Ser.* **29**, 91-100.

Essene, E.J. & Peacor, D.R. (1987): Petedunnite (CaZn Si_2O_6), a new zinc clinopyroxene from Franklin, New Jersey, and phase equilibria for zincian pyroxenes. *Am. Mineral.* **72**, 157-166.

Ewart, A., & Griffin, W.L. (1994): Application of proton-microprobe data to trace-element partitioning in volcanic rocks. *Chem. Geol.* **117**, 251-284.

Fehr, K.T. & Huber, A.L. (2001): Stability and phase relations of $CaZnSi_3O_8$, a new phase with feldspar structure in the system CaO–ZnO–SiO_2. *Am. Mineral.* **86**, 21-28.

Graybeal, F.T. (1973): Copper, manganese, and zinc in coexisting mafic minerals from Laramide intrusive rocks in Arizona. *Econ. Geol.* **68**, 785-798.

Hendry, D.A., Chivas, A.R., Long, J.V., & Reed, S.J. (1985): Chemical differences between minerals from mineralizing and barren intrusions from some North American porphyry copper deposits. *Contrib. Mineral. Petrol.* **89**, 319-329.

________, ________, Reed, S.J.B. & Long, J.V.P. (1982): Geochemical evidence for magmatic fluids in porphyry copper mineralization. II. Ion-probe analysis of Cu contents of mafic minerals, Koloula igneous complex. *Contrib. Mineral. Petrol.* **78**, 404-412.

Holland, H.D. (1959): Stability relations among the oxides, sulfides, sulfates and carbonates of ore and gangue metals. 1. Some applications of thermochemical data to problems of ore deposits. *Econ. Geol.* **54**, 184-233.

________ (1965): Some applications of thermochemical data to problems of ore deposits. 2. Mineral assemblages and the composition of ore forming fluids. *Econ. Geol.* **60**, 1101-1166.

Ilton, E.S. & Veblen, D.R. (1988): Copper inclusions in sheet silicates from porphyry Cu deposits. *Nature* **334**, 516-518.

________ & ________ (1993): Origin and mode of copper enrichment in biotite from rocks associated with porphyry copper deposits: a transmission electron microscopy investigation. *Econ. Geol.* **88**, 885-900.

Jiang, S.-Y., Palmer, M.R., Slack, J.F., Yang, J.-H. & Shaw, D.R. (2000): Trace element and rare earth element geochemistry of tourmalinites and related rocks and ores from the Sullivan Deposit and vicinity, southeastern British Columbia. *In* The Geological Environment of the Sullivan Deposit, British Columbia (J.W. Lydon, T. Hoy, J.F. Slack & M.E. Knapp, eds.). *Geol. Assoc. Can., Spec. Publ.* **1**, 482-495.

John, D.A. (1989): Geologic setting, depths of emplacement, and regional distribution of fluid inclusions in intrusions of the central Wasatch Mountains, Utah. *Econ. Geol.* **84**, 386-409.

________ (1997): Geologic setting and characteristics of mineral deposits in the central Wasatch Mountains, Utah. *In* Geology and Ore Deposits of the Oquirrh and Wasatch Mountains, Utah (D.A. John & G.H. Ballantyne, eds.). *Soc. Econ. Geol., Guidebook Ser.* **29**, 11-34.

________, Turrin, B.D. & Miller, R.J. (1997): New K–Ar and $^{40}Ar/^{39}Ar$ ages of plutonism, hydrothermal alteration and mineralization in the central Wasatch Mountains, Utah. *In* Geology and Ore Deposits of the Oquirrh and Wasatch Mountains, Utah (D.A. John & G.H. Ballantyne, eds.). *Soc. Econ. Geol., Guidebook Ser.* **29**, 47-57.

Katkov, A.E. & Lykasov, A.A. (2003): Spinel phase relations in the Fe_3O_4–$CuFe_2O_4$ system. *Inorganic Materials* **39**, 171-174.

Kesler, S.E., Issigonis, M.J., Brownlow, A.H., Damon, P.E., Moore, W.J., Northcote, K.E. & Preto, V.A. (1975): Geochemistry of biotites from mineralized and barren intrusive systems. *Econ. Geol.* **70**, 559-567.

Kirkpatrick, P. & Baez, V. (1948): Formation of optical images by X-rays. *J. Opt. Soc. Am.* **38**, 766-774.

Li, G., Peacor, D.R. & Essene, E.J. (1998): The formation of sulfides during alteration of biotite to chlorite-corrensite. *Clays & Clay Minerals* **46**, 649-657.

Lovering, T.G., Cooper, J.R., Drewes, H.D. & Cone, G.C. (1970): Copper in biotite from igneous rocks in southern Arizona as an ore indicator. *U. S. Geol. Surv., Prof. Paper* **700-B**, 1-8.

MacDonald, D.J. & Hawthorne, F.C. (1995): Cu-bearing tourmaline from Paraiba, Brazil. *Acta Crystallogr.* **C51**, 555-557.

Parry, W.T. & Nackowski, M.P. (1963): Copper, lead, and zinc in biotites from Basin and Range quartz monzonites. *Econ. Geol.* **58**, 1126-1144.

________, Wilson, P. N., Moser, D. & Heizler, M. T. (2001): U–Pb dating of zircon and ^{40}Ar/^{39}Ar dating of biotite at Bingham, Utah. *Econ. Geol.* **96**, 1671-1683.

Phillips, C.H., Smith, T.W. & Harrison, E.D. (1997): Alteration, metal zoning, and ore controls in the Bingham Canyon porphyry copper deposits, Utah. *In* Geology and Ore Deposits of the Oquirrh and Wasatch Mountains, Utah (D.A. John & G.H. Ballantyne, eds.). *Soc. Econ. Geol., Guidebook Ser.* **29**, 133-145.

Redmond, P.B. (2002): *Magmatic-Hydrothermal Fluids and Copper–Gold Ore Formation at Bingham Canyon, Utah*. Ph.D. dissertation, Stanford University, Stanford, California.

________, Einaudi, M.T., Inan, E.E., Landtwing, M.R. & Heinrich, C.A. (2004): Copper deposition by fluid cooling in intrusion-centered systems: new insights from the Bingham porphyry ore deposit, Utah. *Geology* **32**, 217-220.

Rehrig, W.A. & McKinney, C.N. (1976): The distribution and origin of anomalous copper in biotite. *Mining Engineering* **27**, 68 p.

Rothkopf, A.L. & Fehr, K.T. (1998): The chemical potential of hedenbergite in hedenbergite–petedunnite solid solution determined by EMF measurements. *Terra Abstracts* **10**, *Suppl.* **1**, 53.

Sapozhnikova, E.Ya., Davidovich, A.G., Roizenblat, E.M., Zinovik, M.A., Kosheleva, L.V., Maslova, V.M. & Markovskii, E.V. (1981): Degree of oxidation of cations in a series of solid solutions of the $CuFe_2O_4$–$Cu_{0.5}Fe_{2.5}O_4$–Fe_3O_4 system. *Zh. Neorgan. Khimii* **26**, 1751-1754.

Shannon, R.D. (1976): Systematic studies of interatomic distances in oxides. *In* The Physics and Chemistry of Minerals and Rocks (R.G.J. Strens, ed.). John Wiley & Sons, London, U.K.

Smith, J.V. & Rivers, M.L. (1995): Synchrotron X-ray microanalysis. *In* Microprobe Techniques in the Earth Sciences (P.J. Potts, J.F. Bowles, S.J.B. Reed & M.R. Cave, eds.). Chapman & Hall, London, U.K. (163-233).

Stimac, J. & Hickmott, D. (1994): Trace-element partition coefficients for ilmenite, orthopyroxene and pyrrhotite in rhyolite determined by micro-PIXE analysis. *Chem. Geol.* **117**, 313-330.

Taylor, S.R. & McLellan, S.M. (1985): *The Continental Crust: its Composition and Evolution*. Blackwell Scientific Publications, Oxford, U.K.

Vogel, T.A., Cambray, F.W. & Constenius, K.N. (2001): Origin and emplacement of igneous rocks in the central Wasatch Mountains, Utah. *Rocky Mountain Geol.* **36**, 119-162.

Waite, K. A., Keith, J.D., Christiansen, E.H., Whitney, J.A., Hattori, K., Tingey, D.G., & Hook, C.J. (1997): Petrogenesis of the volcanic and intrusive rocks associated with the Bingham Canyon porphyry Cu–Au–Mo deposit, Utah. *In* Geology and Ore Deposits of the Oquirrh and Wasatch Mountains, Utah (D.A. John & G.H. Ballantyne, eds.). *Soc. Econ. Geol., Guidebook Ser.* **29**, 69-90.

Warnaars, F.W., Smith, W.H., Bray, R.E., Lanier, G. & Shafiqullah, M. (1978): Geochronology of igneous intrusions and porphyry copper mineralization at Bingham, Utah. *Econ. Geol.* **73**, 1242-1249.

Willson, W.H. (1979): *The Distribution of Copper in the Mafic Minerals of the Guichon Creek Batholith*. M.Sc. thesis, Univ. of Toronto, Toronto, Ontario.

Received September 9, 2004, revised manuscript accepted March 31, 2005.